

Jupiter Plasma Wave Observations: An Initial Voyager 1 Overview

Abstract. The Voyager 1 plasma wave instrument detected low-frequency radio emissions, ion acoustic waves, and electron plasma oscillations for a period of months before encountering Jupiter's bow shock. In the outer magnetosphere, measurements of trapped radio waves were used to derive an electron density profile. Near and within the Io plasma torus the instrument detected high-frequency electrostatic waves, strong whistler mode turbulence, and discrete whistlers, apparently associated with lightning. Some strong emissions in the tail region and some impulsive signals have not yet been positively identified.

The Voyager 1 mission provided the first opportunity to examine directly wave-particle interaction phenomena within the magnetosphere of Jupiter and in the extensive region of disturbance upstream from the planet. This report contains an overview of encounter measurements from the Voyager 1 plasma wave investigation for the period starting with initial detection of Jupiter phenomena and ending a few days after closest approach. During this time, the magnetosphere was strongly affected by a dense plasma torus associated with Io (1) and perturbed by changing interplanetary

conditions (2). Some interactions in the Io plasma torus resembled those found in Earth's plasmasphere. This region contained strong whistler mode turbulence (chorus, hiss, and impulsive signals that appear to be associated with lightning). Electrostatic emissions related to the electron gyrofrequency harmonics and upper hybrid resonance were also detected beyond the boundary of the torus and near the magnetic equator crossings. Radio waves trapped between the outer torus region and the dayside magnetopause (continuum radiation) allowed us to determine electron density profiles, as

at Earth (3). The wave-particle interactions at the inbound bow shock and in the upstream region were also structurally similar to those detected near Earth. In addition, the Voyager 1 plasma wave instrument discovered several important Jupiter wave phenomena that have no certain analogs at Earth, such as strong radio emissions in the range 10 to 56 kHz, very intense low-frequency (a few hundred hertz) wave levels at high latitudes in the tail, impulsive electrostatic-type emissions in the inner magnetosphere, and possible signals directly associated with Io.

The plasma wave sensor is a balanced electric dipole with a 7-m effective length. In the normal encounter format the ambient signals are processed with a 16-channel spectrum analyzer (10 Hz to 56 kHz) that provides a full spectral scan every 4 seconds. The Voyager high-rate telemetry (115 kilobits per second) is

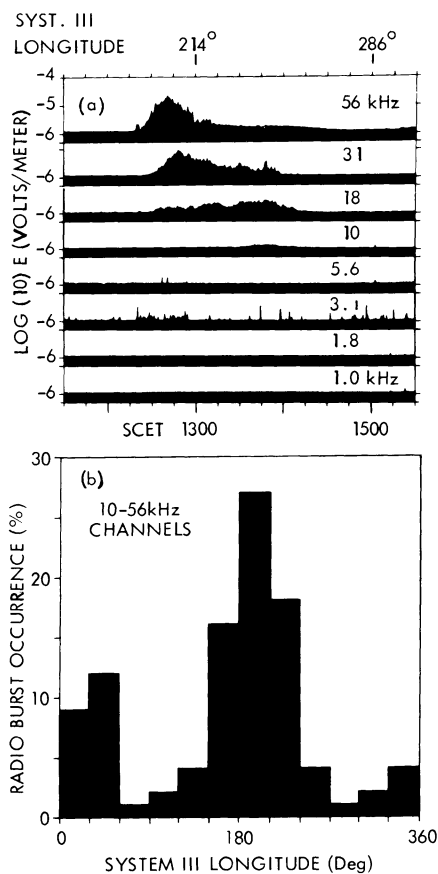


Fig. 1. (a) A radio burst from Jupiter detected on 22 February 1979 at a range of $173 R_J$. The lower cutoff of the radio burst was at 10 kHz, and the observations at 3.1 kHz represented electron plasma oscillations. Spacecraft event times (SCET) are used throughout this report. (b) Distribution of radio burst events with System III longitude for the interval 12 December 1978 through 22 February 1979. The peaks near 210° and 30° are presumably connected with tipping of the north and south magnetic poles of Jupiter toward the spacecraft.

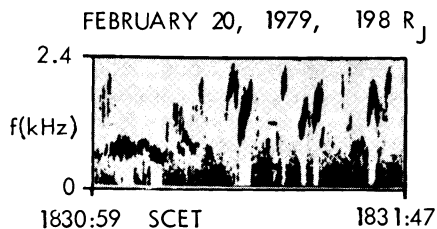


Fig. 2. Ion acoustic waves detected in the upstream solar wind.

used at selected times to record complete wide-band data over the frequency range 50 Hz to 12 kHz. Scarf and Gunnert (4) gave a detailed account of the instrument design and operating characteristics.

A new type of radio emission from Jupiter was first detected in the 10- to 56-kHz channels on 1 October 1978, when Voyager was at 4.27 AU (heliocentric). At large distances, these radio bursts typically lasted for 1 hour or less, and the emission was often sporadic with much fine structure. As Voyager 1 approached Jupiter, the signal level increased and the duration of the detectable emission became longer. Figure 1a shows one event from 22 February 1978 (radius $R = 173 R_J$, where R_J is the Jupiter radius) that exhibited a drift down to lower frequencies. (About 20 percent of these Jupiter radio bursts have appearances generally similar to type III solar radio bursts, and they may be generated by fast electron streams.) Since weak electron plasma oscillations were present in the 3.1-kHz channel, this shows that the 10-kHz lower limit of the radio burst is not related to the local plasma frequency cutoff. It appears that the lower limit is associated with the magnetosheath density barrier, which traps radio waves of frequency $f \leq$ the magnetosheath electron plasma frequency (generally about 5 kHz for Jupiter). These emissions are also detected by the planetary radio astronomy investigation at frequencies comparable to ours and at higher frequencies; the radio measurements show that these waves are not related to the familiar decametric radio emissions. The histogram of Fig. 1b summarizes the distribution of events detected between 12 December 1978 and 22 February 1979, and it shows that these low-frequency bursts were most likely to be detected when one of the Jovian magnetic poles was tipped toward the spacecraft. These intense radio bursts (up to 10^9 W of radiated power in each of our 15 percent bandwidth channels, assuming isotropy) are also distinctive in that they do not exhibit any obvious Io control (5).

In addition to the radio waves and the electron plasma oscillations in the upstream region, occasional bursts of ion acoustic waves were found. Figure 2 shows a short segment of wide-band data from 20 February ($R = 198 R_J$) in which intense ion acoustic waves were clearly present (6).

Jupiter's bow shock was first encountered near spacecraft event time (SCET) 1433 on 28 February, when Voyager 1 was at a range of $85.6 R_J$; the wave observations in the shock region are shown in Fig. 3. Before 1430, upstream electrons produced electron plasma oscillations at 3.1 kHz, and no other significant precursors were detected (the signals in the 100- and 178-Hz channels are interference tones from the stepper motor of the low energy charged particle instrument). This bow shock was well defined (peak turbulence levels in the 30- to 300-Hz channels, of duration 2 to 3 minutes) and surprisingly low noise levels were detected in the magnetosheath, in contrast with the Earth and Venus observations. The 178- to 560-Hz channels had barely perceptible postshock wave level enhancements, and the magnetosheath levels in the 10- to 56-Hz channels were actually lower than those detected upstream.

The shock surface moved out past

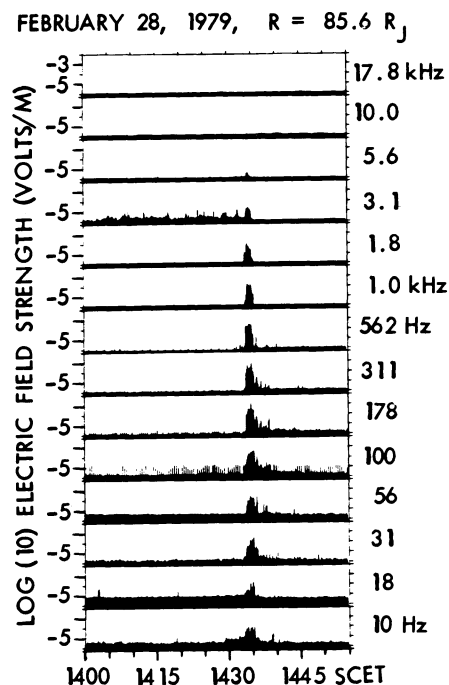


Fig. 3. Measurements of wave amplitudes at the first bow shock crossing. Interference appears in the 100- and 178-Hz channels, and the upstream enhancements at 3.1 kHz represent detection of electron plasma oscillations. Note the very low noise levels in the magnetosheath after 1435.

Voyager 1 at 1953 on 28 February, and it moved in again at 1228 on 1 March. In both cases the plasma wave measurements were similar to those shown in Fig. 3, the main differences being that the second and third crossings were narrower and the upstream electron plasma oscillations now appeared in the 5.6-kHz channel. Throughout the interval from 1433 on 28 February until 1950 on 1 March, the magnetosheath plasma wave turbulence remained exceptionally low.

Figure 4 shows wave observations in the region of the initial magnetopause crossing. Before entry into the magnetosphere the characteristic low magnetosheath wave levels were measured, and the magnetopause detection was marked by the onset of strong continuum radiation (3). Between about 1950 and 2015, the lower limit of the continuum noise decreased smoothly from 5.6 kHz to below 1 kHz. We identify the low-frequency bound of the noise band as the local electron plasma frequency, $f_p = 9000 \sqrt{N}$ Hz (N is the electron density in cm^{-3}). This identification leads to determination of an electron density profile,

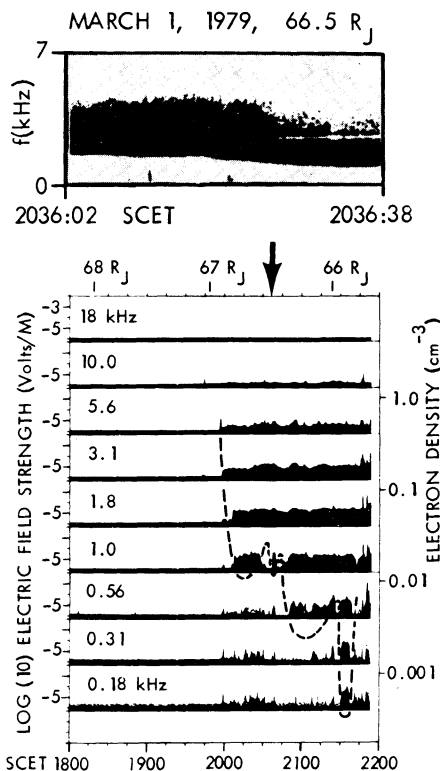


Fig. 4. Detection of continuum radiation after the first magnetopause crossing. The dashed curve is a density profile constructed by assuming that the spectrum is bounded by the electron plasma frequency (see scale on right). The frequency-time diagram at the top shows how the complete wave-form record is used to obtain a precise lower bound for the spectrum, and this gives a very accurate density value.

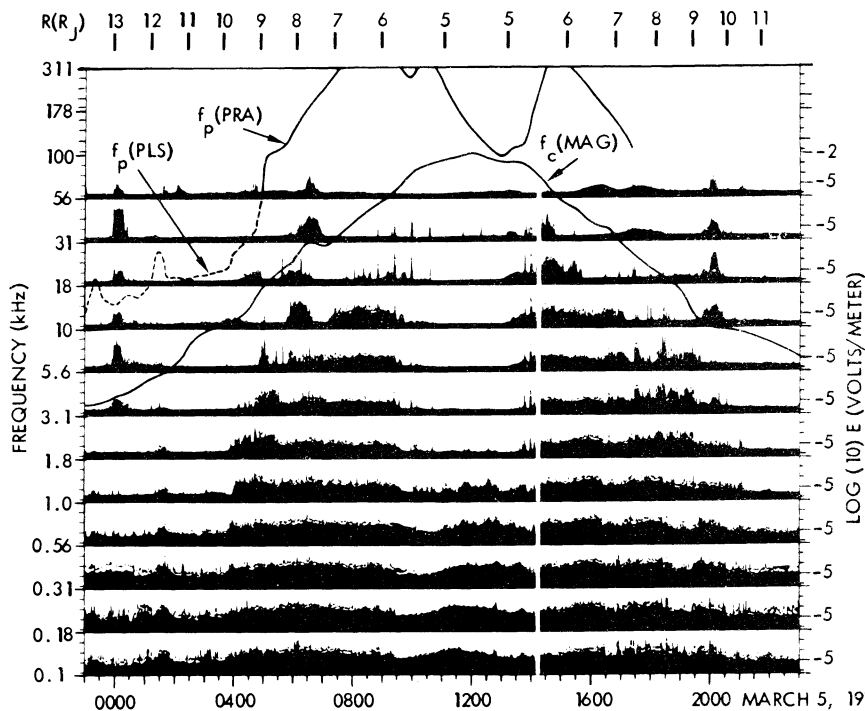


Fig. 5. Plasma wave observations near closest approach, along with preliminary estimates of the electron plasma frequency [determined by the plasma probe (PLS) and the planetary radio astronomy instrument (PRA)] and a preliminary electron cyclotron frequency plot [from the magnetometer (MAG)]. The Io torus (entered at about 0500) contains strong whistler mode turbulence (chorus and hiss) and some signals that appear to be lightning whistlers (for instance, near 0948). Other observations are discussed in the text.

such as the one represented by the dashed curve of Fig. 4 (density scale on the right), which shows large fluctuations and an enormous total range of variation. Our analysis indicates that N was near 0.4 cm^{-3} just within the magnetopause and fell to below $4 \times 10^{-4} \text{ cm}^{-3}$ just after 2130.

The wave-form observations have helped to confirm this mode identification and to resolve questions about the density profile in regions where large variations were present. For instance, near 2030, Fig. 4 shows large changes in the 1-kHz wave level, and the 16-channel data could be interpreted in various ways. Fortunately, the wide-band records, such as the one displayed at the top of Fig. 4, show precisely how to draw the density profile. Specifically, the observed change in the lower edge of the continuum noise band in Fig. 4 tells us that the electron density fell from $2.8 \times 10^{-2} \text{ cm}^{-3}$ at 2036:02 to 7.9×10^{-3} at 2036:38. This type of analysis provides an unambiguous and accurate determination of the electron density. Moreover, since it is based on study of characteristics of a propagation cutoff for radio waves with wavelengths of many kilometers, sheath effects associated with the presence of the Voyager spacecraft within the plasma cannot affect the density evaluation.

This capability is especially important in regions, such as the outer magnetosphere, where the plasma temperature is high. The low energy charged particle instrument found a mean ion temperature of several tens of kilovolts near 2015, with an energetic ion density comparable to the value indicated on Fig. 4 (7), and it is probable that here the plasma was completely described by the energetic particle population.

Voyager continued to traverse the outer magnetosphere-magnetosheath-solar wind region for the next few days, as changing interplanetary conditions strongly perturbed Jupiter's magnetosphere. The magnetopause swept inward

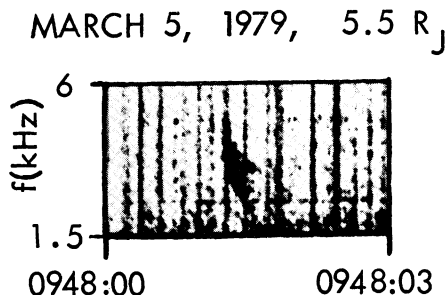


Fig. 6. Example of an impulsive, relatively undispersed signal that has the characteristic form of a lightning whistler. This noise burst was detected as Voyager crossed an apparent density duct, as indicated by the PRA measurement of electron plasma frequency.

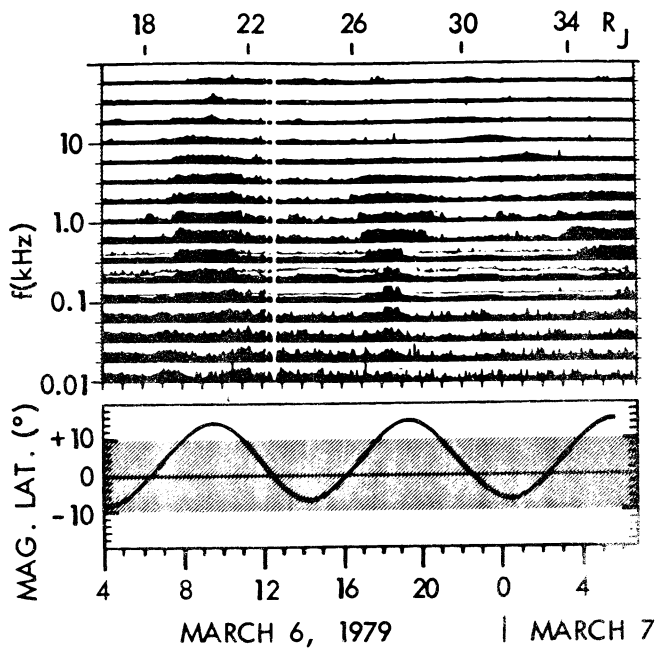


Fig. 7. Intense low-frequency noise detected at high magnetic latitudes ($\approx 10^\circ$) during the second pass.

at about 0740 on 2 March, and Voyager was actually back out in the solar wind between 0950 and 1310 later that day. At about 0230 on 3 March, when Voyager was near $46 R_J$, the spacecraft reentered the magnetosphere. Shortly after 1000 on 3 March the density appeared to increase significantly as Voyager may have been close to (or even within) the magnetosheath again; however, a data gap ending near 1440 ($R \approx 38 R_J$) obscured the situation in this region. After this data gap, Voyager remained within the outer magnetosphere, and during the next 24 hours the plasma wave instrument continued to detect radio emissions, continuum radiation, and increasing levels of low-frequency turbulence similar to electromagnetic hiss.

Clear detection of wave phenomena associated with strong wave-particle interactions did not start until 1400 on 4 March, when Voyager was at a range of $21 R_J$. At 1400, 1900, and 2400, the spacecraft crossed the magnetic equator and fairly strong (maximum electric field strength E_{\max} up to 1 mV/m) emissions at $f \approx 3$ and $5 f_c/2$ were detected (the local electron gyrofrequency f_c equals $28 B$ in hertz, when the magnetic field strength B is expressed in gammas). These electrostatic waves have been found to be concentrated near the equator beyond Earth's plasmasphere, and at Earth the associated wave-particle interactions are thought to produce the diffuse aurora (8). This type of wave-particle interaction at large Jovian distances could contribute to the polar aurora detected by the Voyager ultraviolet spectrometer (1).

The plasma conditions, the energetic particle distributions, and the wave ac-

tivity in the inner magnetosphere were all highly complex and nonuniform, and a full discussion cannot be attempted here. It is useful, however, to point out a few of the main types of observed phenomena, using a compressed plot as a guide. Figure 5 contains 48-second averages (black areas) and peaks (fine lines) for each of the 12 upper plasma wave channels, along with preliminary profiles of the plasma frequency [derived from the PLS plasma probe (2) and the PRA radio receiver (5)] and the cyclotron frequency [derived from the magnetometer data (9)]. The wave plots in Fig. 5 are calibrated in that the top of each panel corresponds to a field strength of 10^{-2} V/m, with additional scale marks shown on the right.

One outstanding open problem in Jupiter's inner magnetosphere involved the concept that the intensities of energetic electrons would be self-limiting because of a whistler mode plasma instability (10). The Pioneer 10 and 11 measurements of "hat-shaped" pitch-angle distributions had been cited as indirect evidence that strong whistler mode turbulence was present (11), especially in the region of the Io orbit, and it is gratifying that Voyager did find these waves within the Io plasma torus, which is clearly defined in Fig. 5 by the broad increases in the f_p curve (rises centered about $6 R_J$). We identify the whistler mode waves as the relatively steady signals that are strong and persistent at low frequencies (extending from 0415 to about 1800 in the 310-Hz channel, with E_{\max} up to 0.1 and 1.0 mV/m) and that come in two groups at higher frequencies (from 0600 to 0930 and from about 1400 to 1700, at 5.6 kHz).

These signals resemble chorus and hiss, and they have high intensities across a broad spectral band when $f_p \gg f_c$ (note the brief period with increased noise at 0140). The decreased levels detected near the inner edge of the Io torus may be associated with the fact that f_p/f_c became small here (the continued appearance of noise below 1 kHz could be related to cross-field propagation for waves with f below the lower hybrid frequency). The observed whistler waves appear to be generally capable of producing the predicted pitch-angle scattering and diffusion (10).

Electrostatic emissions are frequently impulsive rather than steady, and many of the series of bursts shown in Fig. 5 have a structure of this type. In particular, we call attention to the bursty appearance of the 18-kHz noise observed in the Io flux tube (≈ 1500 to 1530) and the strong 1- to 10-kHz emissions detected on the boundary of the Io plasma torus (0400 to 0600, and 1800 to 1930); the sporadic nature of the emissions suggests that they could be electromagnetic or electrostatic waves. It is also very evident that intense electrostatic waves having $f > f_c$ were detected in the inner magnetosphere. Near 0000, 0630, 1700, and 2000, some of the large-amplitude waves appear to be gyrofrequency harmonics with $f \approx 3 f_c/2$, $5 f_c/2$, and so on.

Near closest approach we carried out a search for lightning whistlers, and a number of isolated noise spikes were identified as signals that do have suitable dispersive characteristics. One example of such an impulsive signal with relatively low dispersion is shown in Fig. 6. Approximately 40 whistlers of this type have been detected in the small amount of wave-form data analyzed to date, and we interpret these as lightning whistlers from sources in Jupiter's atmosphere (12), although we cannot yet rule out the possibility that some of the impulsive signals detected in the Io flux tube were generated close to Io. The detection of low-frequency radio signals from atmospheric lightning supports the lightning interpretation of the bright spots detected by the imaging system on the night-side of Jupiter (13).

After closest approach Voyager headed out in a predawn direction (sun-Jupiter-probe angle near 245°) and the spacecraft traversed a fairly regular tail-like region for several days. During this time, intense low-frequency ($f \leq 1$ kHz) plasma waves were detected whenever the spacecraft was at high magnetic latitudes. Several examples are shown in Fig. 7, which contains a compressed 16-channel plot for a 30-hour interval start-

ing soon after closest approach. The peak plasma wave amplitudes were quite high (for example, near 1815 on 6 March, the 56- and 100-Hz wave levels ranged up to about 4 mV/m), and these waves, which have no analogs in Earth's tail region, are presently unidentified. The waves have some characteristics that suggest a relationship with continuum radiation.

This brief report touches on only a few aspects of the plasma wave observations near Jupiter. At the time of writing we had only received data records for a very small fraction of the actual wave-form observations, and the complete analysis of Jovian plasma physics will naturally involve study of all of these samples, as well as detailed correlations with measurements from other Voyager instruments.

FREDERICK L. SCARF

*Space Sciences Department, TRW
Defense and Space Systems Group,
Redondo Beach, California 90278*

DONALD A. GURNETT

WILLIAM S. KURTH

*Department of Physics and Astronomy,
University of Iowa, Iowa City 52242*

References and Notes

1. A. L. Broadfoot *et al.*, *Science* **204**, 979 (1979).
2. H. S. Bridge *et al.*, *ibid.*, p. 987.
3. R. R. Shaw and D. A. Gurnett, *J. Geophys. Res.* **78**, 8136 (1973); D. A. Gurnett, *ibid.* **80**, 2751 (1975); D. A. Gurnett and L. A. Frank, *ibid.* **81**, 3875 (1976).
4. F. L. Scarf and D. A. Gurnett, *Space Sci. Rev.* **21**, 289 (1977).
5. J. W. Warwick *et al.*, *Science* **204**, 995 (1979). Also, W. S. Kurth, D. D. Barbosa, F. L. Scarf, D. A. Gurnett, and R. L. Poynter (in preparation) will give further details about the observations by the plasma wave instrument.
6. W. S. Kurth, D. A. Gurnett, F. L. Scarf, *J. Geophys. Res.*, in press.
7. S. M. Krimigis *et al.*, *Science* **204**, 998 (1979).
8. L. R. Lyons, *J. Geophys. Res.* **79**, 575 (1974). See C. F. Kennel, F. L. Scarf, R. W. Fredricks, J. H. McGehee, and F. V. Coroniti [*ibid.* **75**, 6136 (1970)] for a discussion of the distribution about Earth's magnetic equator.
9. N. F. Ness *et al.*, *Science* **204**, 982 (1979).
10. See, for instance, D. D. Barbosa and F. V. Coroniti, *J. Geophys. Res.* **81**, 4531 (1976); D. D. Sentman and C. K. Goertz, *ibid.* **83**, 3151 (1978).
11. J. A. Van Allen, B. A. Randall, D. N. Baker, C. K. Goertz, D. D. Sentman, M. F. Thomsen, H. R. Flint, *Science* **188**, 459 (1975). See also W. Fillius, C. McIlwain, and A. Mogro-Campero [*Geophys. Res. Lett.* **3**, 33 (1976)] and additional comments by F. L. Scarf and N. L. Sanders [*J. Geophys. Res.* **81**, 1787 (1976)].
12. D. A. Gurnett, R. R. Shaw, R. R. Anderson, W. S. Kurth, F. L. Scarf, in preparation.
13. B. A. Smith *et al.*, *Science* **204**, 951 (1979).
14. We are grateful for the invaluable support we received throughout this mission from many members of the Voyager Project at Jet Propulsion Laboratory (JPL) and at NASA Headquarters. This assistance was outstanding, but we cannot list here the names of all those who deserve thanks. However, we must acknowledge the recent special efforts of A. Lane and R. Poynter of JPL that enhanced the science return from the wide-band channels, and we thank R. West and R. Brechwald of the University of Iowa for their excellent programming support. We also thank H. Bridge, N. Ness, and J. Warwick for providing Voyager data in advance of publication and allowing us to present the observations here.